Chemical Engineering Journal 144 (2008) 509–513

Contents lists available at ScienceDirect

Chemical Engineering Journal

journal homepage: www.elsevier.com/locate/cej

Synthesis and characterization of nano-sized ZnO powders by direct precipitation method

ChangChun Chen*, Ping Liu, ChunHua Lu

College of Materials Science and Engineering, Nanjing University of Technology, No. 5 Xinmofan Road, Nanjing 210009, China

ARTICLE INFO

Article history:
Received 18 April 2008
Received in revised form 11 July 2008
Accepted 18 July 2008

PACS:
61.10.Nz
61.46.+w
78.67.Bf

Keywords:
ZnO
Nanoparticles
Thermal decomposition

ABSTRACT

In this study, the precursor precipitates of Zinc oxide (ZnO) were obtained by a direct precipitation method via the reaction between Zinc nitrate ($Zn(NO_3)_2$) and Ammonium carbonate ($(NH_4)_2CO_3$) in aqueous solutions with proper concentration. X-ray diffraction (XRD) analysis demonstrated that the precursor precipitates of ZnO were $Zn_4(CO_3)(OH)_6{\cdot}H_2O$. Both the Differential thermal analysis (DTA) and the thermal gravimetric analysis (TGA) curves of the precursor precipitates show that no further weight loss and thermal effect were observed at a temperature of above 550 °C. The precursor precipitates of ZnO were subjected to thermal calcinations and finally yielded the nano-sized ZnO powders. The calcined ZnO powders were characterized by XRD, Brunauer–Emmet–Teller analysis (BET), and scanning electron microscope (SEM), respectively. The XRD results indicated that the synthesized ZnO powders had a pure wurtzite structure and the average nano-particle sizes were about 35.2 nm. However, the inconsistency of ZnO particle sizes derived from the BET methods and the XRD analysis indicated that a fraction of nano-sized ZnO powders were in the form of aggregates, which was also verified by SEM and TEM image. In addition, both the SEM image and the TEM photograph demonstrated that the nano-sized ZnO particles were of a pseudo-spherical shape.

1. Introduction

Semiconductor nanoparticles have attracted much attention in recent years due to novel optical, electrical and mechanical properties, which results from quantum confinement effects compared with their bulk counterparts. Among various semiconductor nanoparticles, nano-sized Zinc oxide (ZnO) particles are the most frequently studied because of their interest in fundamental study and also their applied aspects such as in solar energy conversion, varistors, luminescence, photo-catalysis, electrostatic dissipative coating, transparent UV protection films and chemical sensors [1–4]. Hitherto, searching new methodology to synthesize uniform nano-sized ZnO particles is of great importance for both fundamental study and practical application, and thus various methods such as thermal decomposition, chemical vapor deposition, sol-gel, spray pyrolysis, and precipitation have still been developed for the fabrication of nano-sized ZnO particles with uniform morphology and size [5–9]. Among these synthetic routes, precipitation approach compared with other traditional methods provides a facile way for low cost and large-scale production, which does not need expensive raw materials and complicated equipments [10]. Recently, Musić et al. [11] have obtained nano-sized ZnO particles via the thermal decomposition of aggregated $Zn_5(CO_3)_2(OH)_6$, which was directly precipitated from the mixing of $ZnCl_2$ or $Zn(Ac)_2$ (Ac = CH_3COO) solution with Na_2CO_3 solution with proper concentration.

In the present work, a direct precipitation method was employed to synthesize nano-sized ZnO particles using some alternative raw materials, which were different from those used in literatures. The precipitation of $Zn_4CO_3(OH)_6{\cdot}H_2O$ precursors was prepared through a reaction between the Zinc nitrate ($Zn(NO_3)_2$) and Ammonium carbonate ($(NH_4)_2CO_3$) solutions, and then nano-sized ZnO particles were obtained by thermal calcination of the $Zn_4CO_3(OH)_6{\cdot}H_2O$ precursors. The structural characteristics of these nano-sized ZnO particles such as the morphology, crystal type, crystal size, particle shape, particle size distribution, degree of agglomeration were determined by XRD, SEM, TEM and Brunauer–Emmet–Teller analysis, respectively.

2. Experimental

The synthetic procedures for the ZnO particles by direct precipitation method are briefly summarized in Scheme 1. $Zn(NO_3)_2$, $(NH_4)_2CO_3$, ethanol, and de-ionized water were used in the

* Corresponding author. Tel.: +86 2583587242; fax: +86 2583587242.
E-mail address: changchunchen@hotmail.com (C. Chen).

1385-8947/$ – see front matter © 2008 Elsevier B.V. All rights reserved.
doi:10.1016/j.cej.2008.07.047

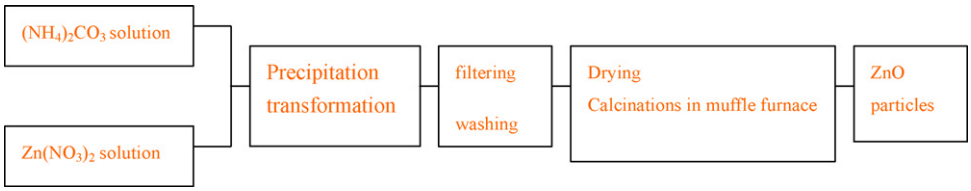

Scheme 1.

experiments. All the reagents used in this study were the analytical grade. $Zn(NO_3)_2$ and $(NH_4)_2CO_3$ were firstly dissolved in high-purity water to form solutions with 1.5 and 2.25 mol/L concentration, respectively. The $Zn(NO_3)_2$ solutions were slowly dropped into the $(NH_4)_2CO_3$ solutions with the vigorously stirring. And then, the precipitates derived from the reaction between the $Zn(NO_3)_2$ and the $(NH_4)_2CO_3$ solutions were collected by filtration and rinsed three times with high-purity water and ethanol, respectively. Subsequently, the washed precipitates were dried at 80 °C to form the precursors of ZnO. Finally, the precursors were calcined at a temperature of 550 °C for 2 h in the muffle furnace to obtain the nano-sized ZnO particles. Some chemical reactions occurred in our preparation process as shown in Scheme 1.

The structural properties of the formed nano-sized ZnO particles were investigated by θ–2θ method of XRD with a Cu Kα_1 (λ = 0.15406 nm) source at 40 kV and 30 mA using a multipurpose XRD system (PANalytical). The morphology and particle size of the nano-sized ZnO particles were also analyzed by a scanning electron microscope (SEM, JXA840). SEM photographs for the nano-sized ZnO particles were recorded (LEO 435) at 30 kV from samples covered with a gold thin film. The morphology and structure of the ZnO nano-sized powders were further investigated by transmission electron microscope (TEM). TEM (JEM-2010) were operated at 200 kV. The specific surface area of nano-sized ZnO particles was determined by nitrogen absorption Brunauer–Emett–Teller (BET) method. The BET measurements were performed on a Micromeritics ASAP 200 instrument. The BET specific surface area 85.0 m^2/g of activated carbon is used as control in experiments. Thermal gravimetric analysis (TGA) curves of the air-dried precursor precipitates were recorded using a TG-DTA/DSC Apparatus (STA449C). Approximately 50 mg of a sample was placed in a platinum crucible on the pan of the microbalance and heated from 50 to 700 °C, using α-Al_2O_3 as inert material. Analysis was performed under flowing nitrogen with a flow rate of 50 mL min^{-1}, and a heating rate of 10 °C min^{-1}.

3. Results and discussion

In order to characterize the nature of the precursor-pyrolysis process, TGA and DTA measurements were carried out. Fig. 1 shows the weight loss of the precursors of nano-sized ZnO particles as a function of temperature. The TGA curve in Fig. 1 shows a major weight loss step at incrementing temperatures from 50 to 220 °C with no further weight loss observed at a temperature up to 700 °C. The weight loss was related to the decomposition of the precursors of ZnO. The clear plateau formed at a temperature between 500 and 700 °C on the TGA curve indicates that the formation of nanocrystalline ZnO was a decomposition product, as confirmed by XRD analysis. On the DTA curve (Fig. 1) a main exothermic effect was observed between 200 and 250 °C with a maximum at about 220 °C, indicating that the thermal events could be associated with the decomposition of the precursors of ZnO. Both no further weight loss and no thermal effect were observed at a temperature above 550 °C, indicating that decomposition does not occur above this temperature and the stable residues are maybe ascribed to ZnO nano-particles.

Fig. 2 depicts XRD pattern of the precursors of ZnO. As we know, the general form of basic zinc carbonate can be written as $mZnCO_3 \cdot nZn(OH)_2 \cdot kH_2O$. As a matter of fact, $Zn_5(CO_3)_2(OH)_6 \cdot H_2O$ and $Zn_4(CO_3)(OH)_6 \cdot H_2O$ of basic zinc carbonate were the well-known forms in previous study [12]. When verify the structure and composition for the basic zinc carbonate, two typical XRD patterns in the database of XRD can be utilized. One is JCPDS 11-287, the other is JCPDS 19-1458. The former corresponds to the XRD pattern of $Zn_5(CO_3)_2(OH)_6 \cdot H_2O$, and the latter denotes the XRD patterns of $Zn_4CO_3(OH)_6 \cdot H_2O$. The XRD patterns shown in Fig. 2 were consistent with the values in the database of JCPDS 11-287. As

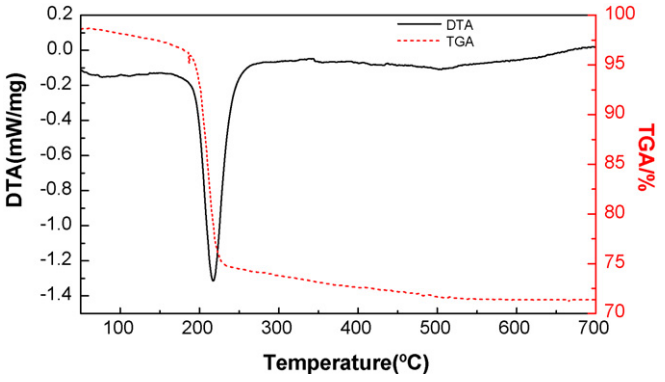

Fig. 1. TGA–DTA curves of the precursors of ZnO.

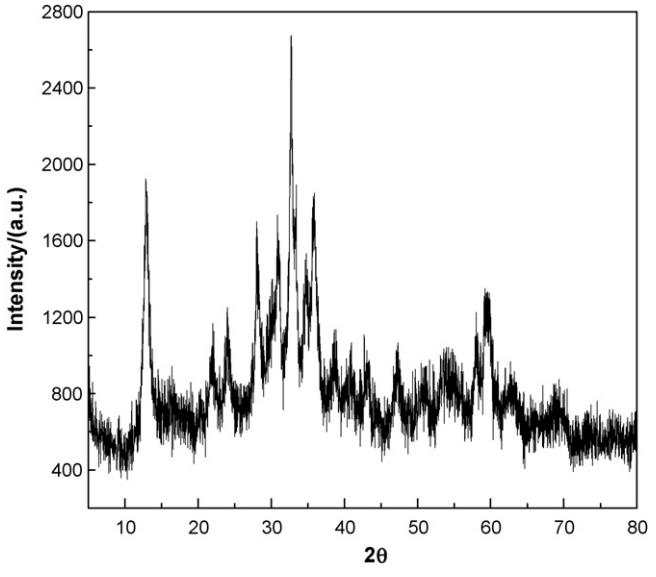

Fig. 2. XRD patterns of the precursors of ZnO.

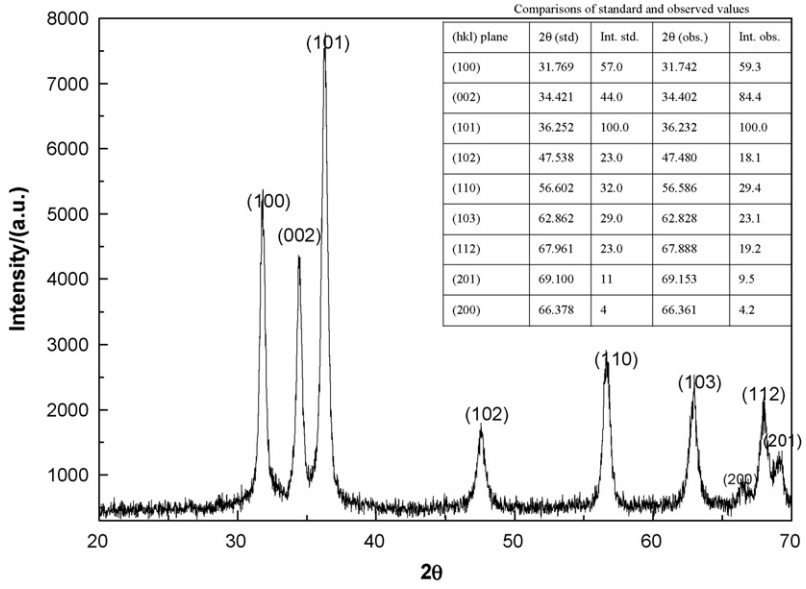

Fig. 3. XRD patterns of the nano-sized ZnO powders.

a consequence, the composition of basic zinc carbonate fabricated in our study was $Zn_4(CO_3)(OH)_6{\cdot}H_2O$.

The XRD patterns of nano-sized ZnO particles obtained from the calcinations of $Zn_4CO_3(OH)_6{\cdot}H_2O$ precursors at a temperature of 550 °C for 2h are shown in Fig. 3. The nano-sized ZnO particles are of a wurtzite structure (hexagonal phase, space group $P6_3mc$). All the diffraction peaks can be well indexed to the hexagonal phase ZnO reported in JCPDS card (No. 36-1451, $a = 0.3249$ nm, $c = 0.5206$ nm). The results indicate that the products were consisted of pure phases. Diffraction peaks related to the impurities were not observed in the XRD pattern, confirming the high purity of the synthesized product. Furthermore, it could be seen that the diffraction peaks shown in Fig. 3 were more intensive and narrower, implying a good crystalline nature of the as-synthesized ZnO product. In addition, the broadening at the bottom of diffraction peaks shown in Fig. 3 also denotes that the crystalline sizes were small and in good agreement with the characteristic of nano-sized particles reported in literature [13]. The average crystalline size (D) of the nano-sized ZnO particles can be obtained from the Debye–Scherrer formula [14],

$$D = \frac{0.89\lambda}{\beta \cos\theta_0} \tag{1}$$

where D is the crystalline size (in nm), λ the wavelength (in nm), β the full width at half maximum (FWHM-in radian) intensity, and θ_0 the Bragg diffraction angle (°). Therefore, the average crystalline size in ZnO powders fabricated from the calcinations of precursor at a temperature of 550 °C for 2 h derived from Eq. (1) was estimated to be about 35.2 nm. In addition, the different diffraction peaks denoted corresponding crystalline planes also were labeled in Fig. 3. On the other hand, the texture coefficient (TC) represents the texture of a particular plane. Quantitative information concerning the preferential crystallite orientation was obtained from the texture coefficient TC($h\,k\,l$) defined as:

$$\mathrm{TC}(h\,k\,l) = \frac{I(h\,k\,l)/I_0(h\,k\,l)}{\sum I(h\,k\,l)/I_0(h\,k\,l)} \times 100\% \tag{2}$$

where $I(h\,k\,l)$ is the measured relative intensity of a plane ($h\,k\,l$), and $I_0(h\,k\,l)$ is the standard intensity of the plane taken from the JCPDS data. The value TC($h\,k\,l$) = 1 represents randomly oriented crystallite, while higher values indicate the abundance of grains oriented in a given ($h\,k\,l$) direction. The observed intensity and the standard intensity of a plane ($h\,k\,l$) are also written in Fig. 3. According to Eq. (2), we can know that the (1 0 0), (0 0 2), and (1 0 1) planes were the preferential crystallite orientation for the nano-sized ZnO particles fabricated in this study.

The specific surface area of the nano-sized powder samples was obtained from the standard Brunauer–Emmett–Teller (BET) procedure. The BET adsorption isotherm equation can be written as follows [15]:

$$\frac{n}{n_\mathrm{m}} = \frac{c(p/p_0)}{(1-p/p_0)(1+(c-1)p/p_0)} \tag{3}$$

where n is the moles of adsorbed gas at p (pressure of adsorbate), c is the BET parameter, n_m is the monolayer capacity in moles, and p_0 is the saturation pressure of the adsorbate. The slope and intercept of the linearized form of the equation give the essential parameters used in determining the surface area. After obtained n according to Eq. (3), the S (specific surface area) value of ZnO powder can be calculated using the following equation [16]:

$$S = nN_\mathrm{A}a_\mathrm{M} \tag{4}$$

where the area that a nitrogen molecular occupies is given by $a_\mathrm{M} = 16.2 \times 10^{-20}\,\mathrm{m}^2$ and Avogadro constant is $N_\mathrm{A} = 6.02 \times 10^{23}\,\mathrm{mol}^{-1}$. As a results, after completing the measurement of BET for the nano-sized ZnO particles, The surface area of the nano-sized ZnO particles fabricated from the calcinations of $Zn_4(CO_3)(OH)_6{\cdot}H_2O$ at a temperature of 550 °C for 2 h is 18.87 m^2/g. This value is in the same range as that reported by Masaki et al. [17], who had utilized zinc sulfate heptahydrate with pulp precursors to prepare ZnO powders. And then, the average crystalline size of nano-sized ZnO powders can be figured out by using the following equation [13]:

$$d_\mathrm{BET} = \frac{6000}{\rho S_\mathrm{BET}} \tag{5}$$

where d_BET is the crystalline size (in nm), ρ is the density of nano-sized ZnO powder (in $\mathrm{g/cm}^3$) and S_BET is the BET specific surface area. In this study, the 56.7 nm of d_BET could be obtained by using the 5.605 $\mathrm{g/cm}^3$ powder density. The inconsistency of ZnO crystalline size determined by the BET methods and the XRD Scherrer formula indicated that there was conglomeration in the nano-sized ZnO

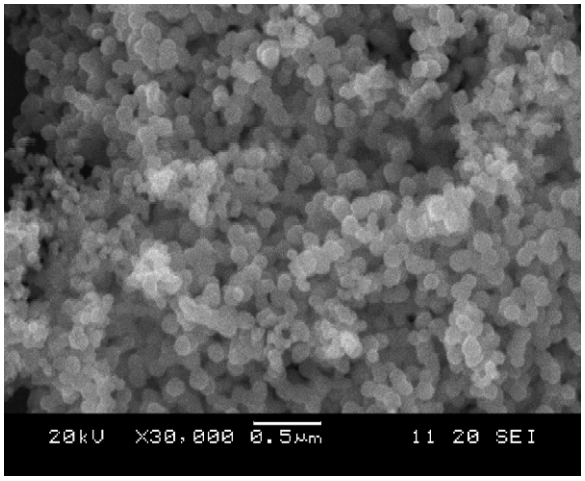

Fig. 4. SEM photograph of the nano-sized ZnO powders.

powders. The agglomeration coefficient can be calculated using the following formula:

$$C_F = \frac{d_{BET}}{D} \quad (6)$$

where C_F is agglomeration coefficient, d_{BET}, D is the average crystalline size determined by the BET methods and the XRD Scherrer formula, respectively. The C_F is bigger, and the agglomeration is more evident. The 1.61 of agglomeration coefficient obtained from Eq. (6) indicates that some conglomerations exist in the nano-sized ZnO powders in our study.

Fig. 4 shows SEM image of the nano-sized ZnO powders resulted from the calcinations of $Zn_4(CO_3)(OH)_6{\cdot}H_2O$ at a temperature of 550 °C for 2h. The morphology of the nano-sized ZnO particles takes on pseudo-spherical shape. The nano-sized ZnO powders obviously show agglomeration of particles, which also agrees with agglomeration coefficient value determined by Eq. (6).

Fig. 5 shows a TEM photograph of ZnO particles obtained from the calcinations of $Zn_4(CO_3)(OH)_6{\cdot}H_2O$ precursors at 550 °C for 2h. TEM indicates that the ZnO particles are approximately spherical and the average diameter of the particles is 32.0 nm. The average particle diameter obtained from the Scherrer formula is 35.2 nm, in good agreement with the value obtained from analysis of transmission electron microscope images. In addition, a fraction of the ZnO nano-sized particles being in the form of aggregates shown in Fig. 5 also agree with those obtained from the SEM image in Fig. 4.

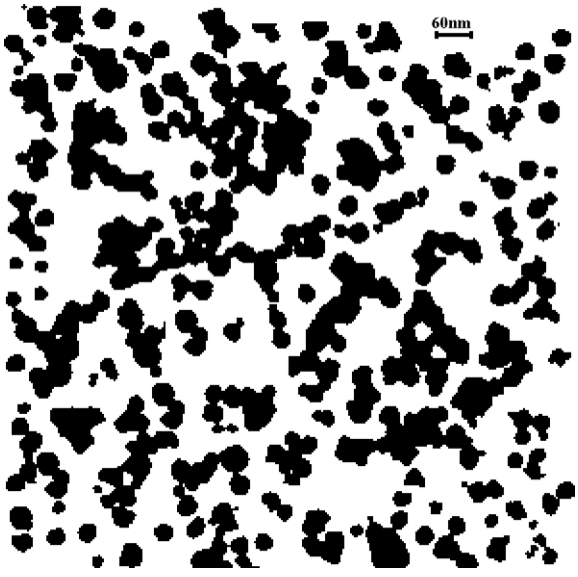

Fig. 5. TEM photograph of ZnO particles obtained from the calcinations of $Zn_4(CO_3)(OH)_6{\cdot}H_2O$ precursors at 550 °C for 2 h.

4. Conclusions

In summary, the nano-sized ZnO particles were prepared by the heat decomposition of the precursors of ZnO with $Zn(NO_3)_2$, $(NH_4)_2CO_3$ as the raw materials. XRD data demonstrated that the precursor of ZnO was $Zn_4(CO_3)(OH)_6{\cdot}H_2O$ and the synthesized nano-sized ZnO particles were of pure wurtzite structures with the average crystalline sizes in 35.2 nm. However, the average crystalline size of ZnO particle obtained from the BET analysis was about 56.7 nm. The inconsistency of the obtained ZnO crystalline size between the XRD analysis and BET analysis maybe indicated that there was conglomeration in the synthesized ZnO powders, which was finally verified by SEM image together with TEM photograph. As we know, the direct precipitation process for the fabrication of the nano-sized ZnO powders is well repeatable and easy controlled, which may offer an attractive strategy for the fabrication of other oxide nano-particles. Consequently, the further improvement in experimental condition for the nano-sized ZnO particles with superfine grain size, good distribution, large specific surface area, and less agglomeration synthesized by direct precipitation is under way.

Acknowledgments

This research was supported by the Science and Technology Foundation of Jiangsu Province under Grant no. bk2006183 and also partially financed by the National Science & Technology Foundation of the Jiangsu Higher education Institute of China, under Grant no. 06KJB430039.

References

[1] Z.L. Wang, J. Song, Piezoelectric nanogenerators based on zinc oxide nanowire arrays, Science 312 (2006) 242–246.
[2] D.C. Look, Recent advances in ZnO materials and devices, Mater. Sci. Eng. B 80 (2001) 383–387.
[3] M. Kitano, M. Shiojiri, Benard convection in ZnO/resin lacquer coating—a new approach to electrostatic dissipative coating, Powder Technol. 93 (1997) 267–273.
[4] I.O. Sosa, C. Noguez, R.G. Barrera, Optical properties of metal nanoparticles with arbitrary shapes, J. Phys. Chem. B107 (2003) 6269–6275.
[5] Y. Yang, H. Chen, B. Zhao, X. Bao, Size control of ZnO nanoparticles via thermal decomposition of zinc acetate coated on organic additives, J. Cryst. Growth 263 (2004) 447–453.
[6] M. Purica, E. Budianu, E. Rusu, M. Danila, R. Gavrila, Optical and structural investigation of ZnO films prepared by chemical vapor deposition (CVD), Thin Solid Films 403–404 (2002) 485–488.
[7] J.H. Lee, K.H. Ko, B.O. Park, Electrical and optical properties of ZnO transparent conducting films by the sol–gel method, J. Cryst. Growth 247 (2003) 119–125.
[8] R. Ayouchi, D. Leinen, F. Martin, M. Gabas, E. Dalchiele, J.R. Ramos-Barrado, Preparation and characterization of transparent ZnO thin films obtained by spray pyrolysis, Thin Solid Films 426 (2003) 68–77.
[9] Z.M. Dang, L.Z. Fan, S.J. Zhao, C.W. Nan, Preparation of nanosized ZnO and dielectric properties of composites filled with nanosized ZnO, Mater. Sci. Eng. B 99 (2003) 386–389.
[10] C. Wang, W.X. Zhang, X.F. Qian, X.M. Zhang, Y. Xie, Y.T. Qian, A room temperature chemical route to nanocrystalline PbS semiconductor, Mater. Lett. 40 (1999) 255–258.
[11] S. Musić, A. Šarić, S. Popović, Dependence of the microstructural properties of ZnO particles on their synthesis, J. Alloys Compd. 448 (2008) 277–283.
[12] D. Klissurski, I. Uzunov, K. Kumbilieva, Preparation of highly dispersed zinc oxide by thermal decomposition of basic zinc carbonate, Thermochim. Acta 93 (1985) 485–488.
[13] C. He, T. Sasaki, Y. Shimizu, N. Koshizaki, Synthesis of ZnO nanoparticles using nanosecond pulsed laser ablation in aqueous media and their self-assembly towards spindle-like ZnO aggregates, Appl. Surf. Sci. 254 (2008) 2196–2202.

[14] C. Chen, B. Yu, J. Liu, Q. Dai, Y. Zhu, Investigation of ZnO films on Si(111) substrate grown by low energy O^+ assisted pulse laser deposited technology, Mater. Lett. 61 (2007) 2961–2964.
[15] C.S. Khachikian, T.C. Harmon, Effects of nonvolatile organic contamination on the surface areas and adsorption energetics of porous media, Langmuir 16 (2000) 9819–9824.
[16] A.L. McCellan, H.F. Honsberger, Cross-sectional areas of molecules adsorbed on solid surfaces, J. Colloid Interface Sci. 23 (1967) 577–599.
[17] K.D. Kim, D.W. Choi, Y.-H. Choa, H.T. Kim, Optimization of parameters for the synthesis of zinc oxide nanoparticles by Taguchi robust design method, Colloids Surf. A: Physicochem. Eng. Aspects 311 (2007) 170–173.